Malaysian Journal of Chemistry, 2026, Vol. 28(2), 203-223

Optimizing Removal of Lead(II) Ions using Spent Coffee Grounds via Response Surface Methodology

Mac Michael M. Rubio*
Department of Physical Sciences, College of Science, University of the Philippines Baguio, Governor Pack Road, Baguio City, Benguet 2600, Philippines
*Corresponding author (e-mail: mmrubio1@up.edu.ph or macmichael_rubio@yahoo.com)

Water pollution caused by heavy metals such as lead poses a serious global threat to both environmental and human health. This study evaluated the effectiveness of untreated spent coffee grounds (SCG) as a low-cost and eco-friendly adsorbent for removing lead(II) from aqueous solutions. Key adsorption parameters such as initial lead concentration, pH, and adsorbent dosage were optimized using response surface methodology (RSM) based on a Box-Behnken design. All parameters and some of their higher-order interactions significantly influenced lead removal. Under optimal conditions of 100 ppm initial lead concentration, pH 5.54, and 10.00 g/L adsorbent dosage, 97.53 % lead removal was achieved upon experimental validation, closely matching the 100 % removal predicted by the RSM model confirming its reliability. SCG also showed comparable performance to activated carbon, which had a 97.05 % removal efficiency. Characterization through ATR-FTIR and SEM-EDS confirmed lead adsorption onto SCG surfaces. The process followed the Langmuir isotherm model and pseudo-second-order kinetics with a maximum adsorption capacity of 68.03 mg/g. These findings highlight SCG's potential as a sustainable alternative for lead(II) remediation in contaminated water systems.

Keywords: Spent coffee grounds, lead(II), removal, adsorption, response surface methodology, waste valorisation

Received: September 2025; Accepted: February 2026

Water is essential for the survival of life. It plays a vital role in sustaining healthy ecosystems and ensuring sufficient food and energy production [1, 2]. However, water contamination has emerged as one of the most pressing global environmental challenges in recent years. The availability of clean and safe water has been increasingly compromised by heavy metal pollution, particularly lead, which poses serious threats to both water quality and water security worldwide [3, 4, 5, 6, 7, 8].

Various techniques have been utilized to eliminate heavy metals from polluted waterways, typically involving chemical and biological processes such as ion exchange, reverse osmosis, electrochemical treatment, and adsorption onto activated carbon [9]. Despite their widespread use, many of these procedures have certain drawbacks and limitations, including high costs, significant chemical requirements, long processing times, incomplete removal, the production of large quantities of toxic sludge, and the creation of non-biodegradable byproducts [10]. In contrast, adsorption is a simple, low-cost, and highly effective treatment process for the removal of heavy metals [9, 10, 11, 12, 13]. One of the potential adsorbent materials that can be used is spent coffee grounds (SCG).

SCG is a waste product generated during the processing of coffee grounds. It consists of the powdered organic residues left behind after hot, high-pressure steam is used to extract coffee from beans. The International Coffee Organization (ICO) reports that global coffee production is increasing due to rising consumer demand, driven primarily by the functional and health-promoting properties of coffee-based food products. This large global production of coffee also generates a significant amount of SCG, which can be used as an adsorbent for the removal of heavy metals from water [14]

An adsorbent's capacity for adsorption is highly dependent on several variables, including solution pH, temperature, contact time, and adsorbent dosage [15]. Typically, when using conventional methods to investigate the adsorption process, one independent variable is changed while the other factors remain constant. However, this approach fails to demonstrate the cumulative effect of all contributing factors simultaneously. Moreover, these methods are often time-consuming and require numerous trials, making it difficult to identify optimal conditions. To address these limitations, response surface methodology (RSM), based on statistical experimental design, has been widely employed to optimize all influencing factors simultaneously [16]. Thus, RSM can be used

as an effective tool to maximize the efficiency of SCG in removing heavy metals from aqueous solutions.

RSM is a statistical and mathematical tool widely used in chemical, pharmaceutical, food, and industrial applications to optimize processes within a given system [17, 18]. It employs appropriate experimental designs with multiple independent variables and uses experimental data to create a model that predicts responses based on key independent factors [19]. RSM also allows for designs with fewer experimental runs without compromising the quality of the outcomes, thus saving time, money, and resources [20, 21].

Numerous studies have successfully applied RSM to optimize various parameters for the adsorption of heavy metals onto different adsorbent materials. For example, Rezaei et al. (2022) [22] employed RSM using a Box-Behnken Design to evaluate the influence of various independent variables including contact time, pH, salinity, initial concentration, biosorbent dosage, temperature, and particle size on the sorption capacity of bivalve mollusc shells and fish scales for lead removal from aqueous solutions. Among the seven factors analysed, biosorbent dosage, initial concentration, and pH were found to have significant effects on all response variables, whereas biosorbent particle size showed no significant impact on any of the responses. Notably, initial concentration emerged as the most influential factor in the lead adsorption process. Similarly, Sun et al. (2014) [16] optimized the adsorption of lead(II) onto modified litchi pericarp (MLP) using RSM, considering contact time, adsorbent dosage, and pH as the key operating parameters. The results demonstrated that MLP achieved a remarkably high adsorption efficiency of 99.97 % for lead(II), with optimal conditions determined at a contact time of 71.56 minutes, an initial pH of 6.81, and an adsorbent dosage of 3.80 g/L. Bahrami et al. (2018) [23] also applied RSM to optimize the removal of lead(II) from water using starch-based adsorbents. The optimal conditions for achieving maximum lead removal efficiency (99.99 %) were identified as a pH of 5.50, temperature of 37.5 °C, initial lead concentration of 63.57 mg/L, adsorbent dosage of 0.25 g, and a contact time of 10 minutes.

Although several studies have investigated the use of SCG for lead(II) removal [24, 25, 26], none have integrated response surface methodology (RSM) as an optimization tool. In contrast, the present study applies RSM to optimize lead(II) removal using untreated SCG, thereby establishing the study's novelty and addressing a clear methodological gap in the literature. Guided by previous findings, the present study hypothesizes that lead(II) removal efficiency can be significantly improved by optimizing key operational parameters, and that an appropriate response surface model will adequately describe the relationships among these variables.

Therefore, the present study investigates the potential of SCG, without any pre-treatment, as a low-cost, sustainable, and eco-friendly adsorbent material for the removal of lead(II) from aqueous solutions, and optimizes adsorption parameters such as initial lead concentration, pH, and adsorbent dosage using RSM. Additionally, adsorption kinetics and isotherms were studied to understand the mechanism of lead(II) adsorption onto SCG.

EXPERIMENTAL

Chemicals and Reagents

All chemicals and reagents, including lead(II) nitrate, hydrochloric acid, sodium hydroxide, and nitric acid, were of analytical grade, ACS grade, or HPLC grade, and were purchased from Sigma-Aldrich (St. Louis, MO, USA), Thermo Fisher, or Merck (Darmstadt, Germany).

Sample Collection and Processing

Ground coffee (*Coffee Arabica L.*) beans were purchased from a local coffee shop at Baguio City Market, Benguet, Philippines, and brewed to collect the spent coffee grounds. The grounds were boiled and washed several times with distilled water until the washings were clear. They were then dried in an oven at 100 °C for 24 hours to remove all moisture. Afterward, the dried coffee grounds were pulverized using a blender and passed through an 850-micron laboratory sieve to obtain finer and more uniform particles. The processed grounds were placed in a polyethylene plastic bag, sealed, and stored in a desiccator until use. Activated carbon, used as a positive control, was purchased from a local shop in Baguio City.

Preparation of Lead(II) Solutions

A 1000 ppm stock solution of lead(II) was prepared by dissolving 1.598 g of lead(II) nitrate in 100 ml of distilled water and diluting it to 1000 ml. Working solutions were prepared by diluting the 1000 ppm stock solution with distilled water to the desired concentrations. The pH of each of these solutions was adjusted using 0.1 M HCl or NaOH, and monitored using a pH meter (APERA Instruments PH 850; resolution ±0.01 pH). These solutions were standardized using Atomic Absorption Spectroscopy (AAS) to accurately determine their precise concentrations.

Table 1. Independent variables and their values for Box-Behnken experimental design.

Independent variables	Factors	Units	Levels		
			-1	0	1
Initial lead concentration	A	ppm	100	300	500
pH	B	pH	2.00	4.00	6.00
Adsorbent dosage	C	g/L	1.00	5.50	10.00

Table 2. Experimental design matrix based on Box-Behnken design and corresponding responses.

Run	Independent variables			Response (% Total removal efficiency)
	Initial lead concentration (ppm)	pH	Adsorbent dosage (g/L)	
1	100	2.00	5.50	20.98
2	500	2.00	5.50	6.96
3	100	6.00	5.50	84.22
4	500	6.00	5.50	27.55
5	100	4.00	1.00	57.81
6	500	4.00	1.00	11.63
7	100	4.00	10.00	83.21
8	500	4.00	10.00	36.44
9	300	2.00	1.00	8.03
10	300	6.00	1.00	29.94
11	300	2.00	10.00	6.42
12	300	6.00	10.00	60.70
13	300	4.00	5.50	39.41
14	300	4.00	5.50	31.95
15	300	4.00	5.50	41.36
16	300	4.00	5.50	43.95
17	300	4.00	5.50	45.90
18	300	4.00	5.50	43.95
19	300	4.00	5.50	42.01
20	300	4.00	5.50	39.25
21	300	4.00	5.50	42.98
22	300	4.00	5.50	44.76

Lead(II) Adsorption onto SCG

A specific amount of SCG was weighed into a 15 ml centrifuge tube and soaked with 10 ml of a lead(II) solution of known concentration and pH. The mixture was then stirred using a vortex mixer and shaken in a shaker incubator at 100 rpm and 25 ℃ for a specified time in each run. After the contact period, the supernatant was collected by filtering the mixture through filter paper. These experiments were performed alongside a positive control (activated carbon) and a negative control (without any adsorbent). The resulting supernatant, along with the original lead(II) solution, was diluted within the range of Atomic Absorption Spectroscopy (AAS) lead(II) standards using 1.5 % nitric acid. The actual initial and final concentrations of lead(II) in the supernatant were measured using AAS. The total lead removal efficiency (%) and adsorption capacity of the SCG were calculated using the formulas provided below.

$$Total\ Lead\ Removal\ Efficiency\ (\%) = \frac{C_i - C_f}{C_i} * 100$$

where: C_i= initial lead concentration; C_f= final lead concentration

$$Adsorption\ Capacity\ \left(\frac{mg}{g}\right) = \frac{C_i - C_e}{m} * V$$

where C_i = initial lead(II) concentration in ppm; C_e=equilibrium lead(II) concentration in ppm; V=volume of lead(II) solution in L; and m=mass of SCG in g

RSM Optimization based on Box-Behnken Experimental Design

The Box-Behnken Design (BBD), a subset of RSM, was employed to determine the optimum conditions for the removal of lead(II) by SCG. The independent variables and corresponding values for the experimental design are shown in Table 1. Each variable was varied at three levels: -1, 0, and 1, representing low, middle, and high levels, respectively. The initial lead concentration was varied from 100 to 500 ppm, while the pH of each solution was adjusted between 2.00 and 6.00. The adsorbent dosage ranged from 1.00 to 10.00 g/L, with 0.01 to 0.1 ± 0.0005 g of SCG used for every 10 ml of lead(II) solution of known concentration and pH.

The experimental design matrix consisted of 12 runs at various levels and 10 replicates at centre points, as shown in Table 2. These runs were performed to determine the total lead removal efficiency for each experiment. The experimental data were then used to evaluate the RSM model and optimize the process. This involved determining the significance of each variable and their interactions, analysing the response of the statistically designed experimental matrix, estimating coefficients, predicting the response and equation for the suggested model, and verifying the model's adequacy. The model may be used to calculate the response function and evaluate system performance at any experimental point [27].

The behaviour of the system can be described by an empirical second-order polynomial model, where the response y is partitioned into linear, interactive, and quadratic components. The experimental data were fitted to the following second-order regression equation:

$$y = \beta 0 + \sum_{i=1}^{3} \beta iXi + \sum_{i=1}^{3}\sum_{j=1}^{3} \beta ijXiXj + \sum_{i=1}^{3} \beta iiXi^2$$

Here, y represents the estimated response surface function or the total lead removal efficiency, $\beta 0$ corresponds to the model constant or the value of y if the effects of all independent variables are zero, Xi represents the independent variables (A, B, C), and βi, βii, and βij represent the linear, quadratic, and cross-product coefficient, respectively.

The experimental design and statistical analysis were performed using Stat-Ease 360 software version 23.1.6 (Stat-Ease Inc., Minneapolis, MN 55413, USA). An analysis of variance (ANOVA) was conducted to determine the significance of the model at a 5 % significance level ($p \leq 0.05$). The experimental validity of the model was assessed by comparing the experimental values with the predicted values.

SCG Characterization

The ATR-FTIR spectra of SCG samples before and after adsorption were obtained to determine changes in absorbance and shifts in functional group peak values. These measurements were conducted using an Agilent Cary 630 ATR-FTIR system equipped with a diamond ATR and a thermoelectrically cooled deuterated triglycine sulfate (dTGS) detector. Each spectrum was recorded at a resolution of 4 cm^{-1} with 32 accumulated scans and normalized to the blank obtained from 32 scans collected from an empty ATR cell. All spectra were collected over a spectral range of 4000 to 650 cm^{-1} using MicroLab PC software and further processed with KnowItAll Informatics System 2024 software.

The surface morphology and chemical composition of SCG before and after adsorption were analyzed using a JEOL JSM IT500HR/LA Schottky Field Emission Scanning Electron Microscope (SEM) with Energy Dispersive X-ray Spectroscopy (EDS) capabilities. The SCG samples were placed onto a cleaned silicon wafer and coated with an approximately 8 Å platinum layer using a JEOL JEC-3000 FC auto fine coater. The samples were then imaged at an accelerating voltage of 3 kV and a magnification of 2,500x, and their elemental composition was analyzed for the percentage weight and atoms of several elements. The Pb weight and atom percentages of the SCG samples before and after adsorption were compared to confirm the adsorption of lead(II) onto the SCG surface.

Adsorption Kinetics

The kinetics of lead(II) adsorption onto the surface of SCG were evaluated by performing a series of adsorption experiments at different time intervals. First, 0.1000 ± 0.0005 g of SCG was weighed and

placed in a 15 ml centrifuge tube. Approximately 10 ml of a 250 ppm lead(II) solution (pH = 5.20) was then added to the tubes. The mixture was placed in a vortex mixer, followed by an incubator shaker at 100 rpm and 25 °C for 5, 10, 15, 20, 30, 60, 120, and 150 minutes. After each specified time interval, the samples were removed from the incubator shaker and filtered through filter paper. The resulting supernatant, along with the original lead(II) solution, was diluted to fall within the range of AAS lead(II) standards using 1.50 % nitric acid, and then analysed for lead(II) content using AAS. The experiments were performed in triplicate to ensure reproducibility of the results. The adsorption capacity of all samples and other kinetic parameters was calculated and used to plot first-order and pseudo-second-order kinetic equations. The equation that provided the best fit, as indicated by the highest R^2 value, was used to describe the kinetics of lead(II) adsorption onto SCG.

Adsorption Isotherms

The adsorption isotherm studies of lead(II) onto the surface of SCG were performed to evaluate the mechanism of lead(II) adsorption and to determine the maximum amount of lead(II) that could be adsorbed. The experiments involved varying the lead(II) concentrations from 10 to 300 ppm. Initially, 0.0100 ± 0.0005 g of SCG was weighed and placed in a 15 ml centrifuge tube. Approximately 10 ml of lead(II) solution (pH = 5.20) at the specified concentration was added to the tubes. The mixture was then stirred using a vortex mixer and shaken in an incubator shaker at 100 rpm and 25 °C for 60 minutes. The samples were then removed from the incubator shaker and filtered through filter paper. The resulting supernatant, along with the original lead(II) solution, was diluted to fall within the range of AAS lead(II) standards using 1.50 % nitric acid and analysed for lead(II) content using AAS. The experiments were conducted in triplicate to ensure reproducibility of the results. The adsorption capacity values of all samples were calculated and used to plot linearized Langmuir and Freundlich isotherms. Isotherm parameters were derived from these plots to describe the adsorption process. The isotherm model that provided the best fit, as indicated by the highest R^2 value, was used to describe the adsorption isotherm of lead(II) onto SCG.

RESULTS AND DISCUSSION

RSM Optimization of Adsorption Parameters

Development of Regression Model Equation

BBD, a type of RSM, was used to optimize the adsorption parameters for removing lead(II) from aqueous solutions using spent coffee grounds. The independent variables in this method were the initial lead concentration, solution pH, and adsorbent dosage. Each factor was coded as A, B, and C, respectively, and examined at three levels: low (-1), middle (0), and high (1). The arrangement of the BBD, along with the experimental responses, are shown in Table 2. It consisted of 22 runs: 12 runs for samples at various levels and 10 centre points.

BBD was chosen for its high efficiency, as it requires fewer runs, making it more cost-effective. Additionally, BBD is advantageous when testing factor combinations is expensive or impractical due to physical process constraints. This is because the design points remain within safe operating limits, avoiding the vertices of the cubic region [28].

Various tests, including the sequential model sum of squares, lack of fit tests, and model summary statistics, were performed to assess the adequacy of the model based on the obtained data. The results are presented in Table 3.

The p-value obtained for the quadratic versus 2FI model was 0.0002, indicating a high degree of significance. The model summary statistics showed that the quadratic model was the best fit, as the R^2 = 0.9712 and adjusted R^2 = 0.9496 values were higher compared to other models. The cubic model was disregarded because it was aliased, meaning that the effects of higher-order interactions were combined in the cubic model. Similarly, the lack of fit tests also indicated that the quadratic model was the best fit. In summary, the sequential model sum of squares, lack of fit tests, and model summary statistics showed that the quadratic model was the best fit.

Subsequently, a quadratic polynomial equation was established to assess the total lead removal efficiency of SCG, expressed as follows:

$$Coded\ Equation\ for\ Total\ Lead\ Removal\ Efficiency\ (\%) = 41.21 - 20.46 * A + 20.00 * B + 9.92 * C - 10.66 * AB + 8.09 * BC + 6.93 * A^2 - 14.07 * B^2$$

Table 3. Adequacy results of the response surface model for the removal of lead(II) by SCG adsorption.

Source	Sum of squares	df	Mean square	F-value	p-value	
Sequential model sum of squares						
Mean vs total	32795.76	1.00	32795.76			
Linear vs mean	7335.73	3.00	2445.24	21.62	< 0.0001	
2FI vs linear	716.79	3.00	238.93	2.72	0.0817	
Quadratic vs 2FI	1049.55	3.00	349.85	15.56	0.0002	**Suggested**
Cubic vs quadratic	124.66	3.00	41.55	2.58	0.1185	Aliased
Residual	145.08	9.00	16.12			
Total	42167.57	22.00	1916.71			
Lack of fit tests						
Linear	1891.00	9.00	210.11	13.03	0.0004	
2FI	1174.21	6.00	195.70	12.14	0.0007	
Quadratic	124.66	3.00	41.55	2.58	0.1185	**Suggested**
Cubic	0.00	0.00				Aliased
Pure error	145.08	9.00	16.12			
Source	**Std. dev.**	**R^2**	**Adjusted R^2**	**Predicted R^2**	**Press**	
Model summary statistics						
Linear	10.64	0.7827	0.7465	0.5850	3889.43	
2FI	9.38	0.8592	0.8029	0.4112	5518.57	
Quadratic	4.74	0.9712	0.9496	0.7681	2173.68	**Suggested**
Cubic	4.01	0.9845	0.9639		*	Aliased

This equation can be used to predict the total lead removal efficiency of the process by substituting the given codes of independent variables to the coded equation, which allows observation of the effects of various experimental values on the response. In the above equation, the values of the coefficient indicate the influence of a specific variable on the response, with a positive value representing a synergistic effect, while a negative value suggests an antagonistic effect [29]. The coefficients for B (pH), C (adsorbent dosage), BC (2F interaction effects) and A^2 (quadratic effects) were all positive, indicating that the removal efficiency increased with their values. In contrast, the negative values for other factors, such as A (initial concentration), AB, and B^2 suggested that the removal efficiency decreased as these factor levels increased. Additionally, higher coefficients for A and B compared to C indicated that A and B had a greater impact on lead removal efficiency.

Quadratic Model Analysis of Variance (ANOVA)

Table 4 presents the ANOVA results of the quadratic model for estimating lead(II) removal efficiency. The quadratic regression model contained significant terms, demonstrating its high significance, as indicated by the Fisher's F-test with a high F-value and a low p-value ($F = 64.95$, $p < 0.0001$) [30]. The linear terms A, B, and C, interaction terms AB and BC, and quadratic terms A^2 and B^2 were found to be significant ($p < 0.05$, F-value = 11.66-167.41). This suggests that each factor within the given range had a significant effect on the overall lead removal efficiency of the process as shown in Figure 1. Higher-order interactions, especially between AB and BC, also positively influenced the response, implying that changes in both variables could significantly affect the response, even when other variables remained constant. The significant quadratic terms A^2 and B^2 suggest that the

optimal conditions lay near or within the experimental range of the independent variables. The not significant lack of fit also implies that the model fit the experimental data well.

The R^2 value of 0.9701 indicates that the model accounted for 97 % of the variation in total lead removal efficiency, with roughly 3% attributed to noise. The adjusted R^2 value corrected the R^2 for the sample size and the number of terms in the model. With an adjusted R^2 of 0.9552, the model showed a strong correlation between the observed and predicted values. The predicted R^2 and adequate precision were 0.8879 and 30.0068, respectively. Adequate precision measures the signal-to-noise ratio, with a value greater than 4 being desirable; the result confirmed an adequate signal.

Table 4. ANOVA results of the quadratic model for the estimation of lead(II) removal efficiency.

Source	**Sum of squares**	**df**	**Mean square**	**F-value**	**p-value**	
Model	9091.85	7.00	1298.84	64.95	< 0.0001	Significant
A-Initial lead concentration	3347.69	1.00	3347.69	167.41	< 0.0001	
B-pH	3200.61	1.00	3200.61	160.05	< 0.0001	
C-Adsorbent dosage	787.44	1.00	787.44	39.38	< 0.0001	
AB	454.73	1.00	454.73	22.74	0.0003	
BC	261.97	1.00	261.97	13.10	0.0028	
A^2	233.21	1.00	233.21	11.66	0.0042	
B^2	961.41	1.00	961.41	48.08	< 0.0001	
Residual	279.96	14.00	20.00			
Lack of fit	134.88	5.00	26.98	1.67	0.2364	Not significant
Pure error	145.08	9.00	16.12			
Cor total	9371.81	21.00				
R^2 - 0.9701		Predicted R^2 - 0.8879				
Adjusted R^2 - 0.9552		Adequate precision - 30.0068				

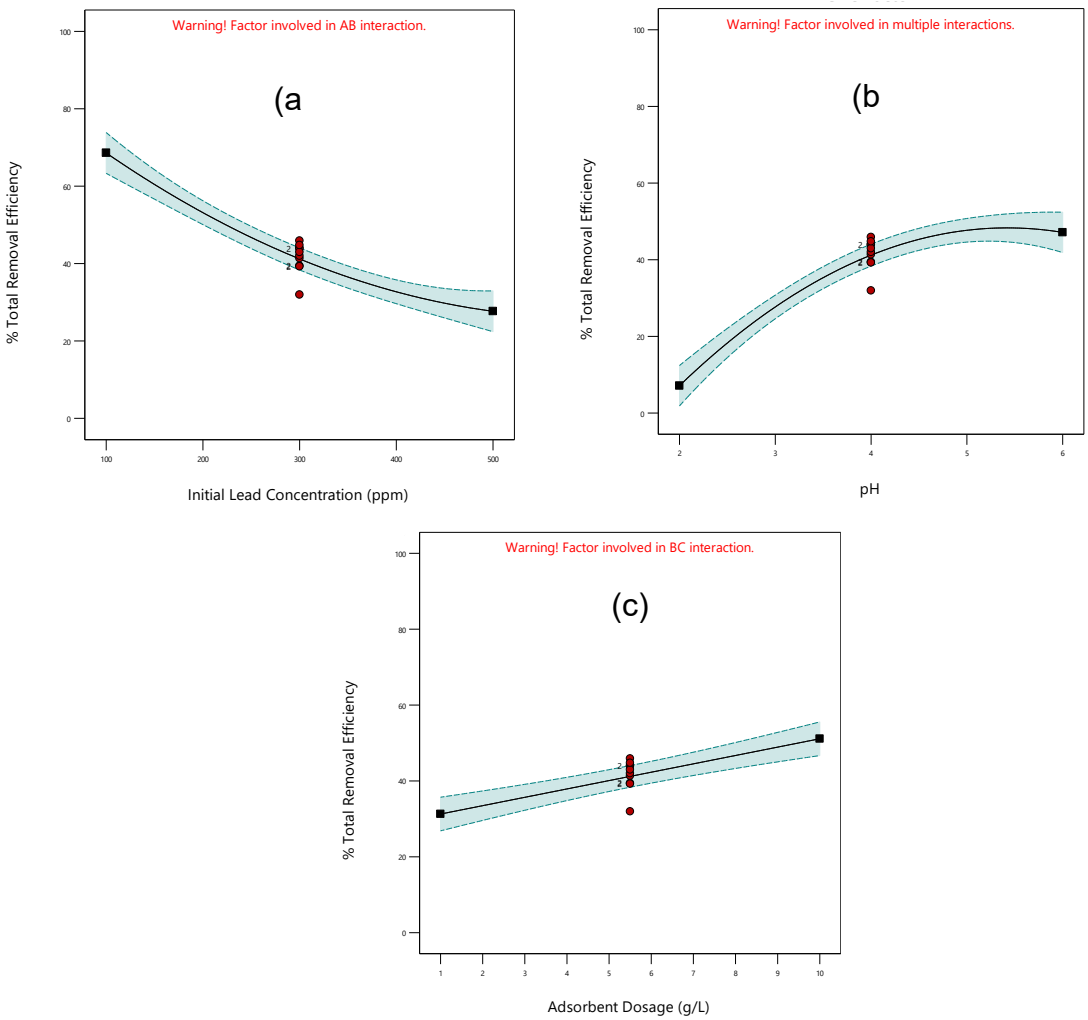

Figure 1. Effects of (a) initial lead concentration, (b) pH, and (c) adsorbent dosage, on the % total removal efficiency based on the Box-Behnken model. Note: red dots in the middle of the graph correspond to the centre points.

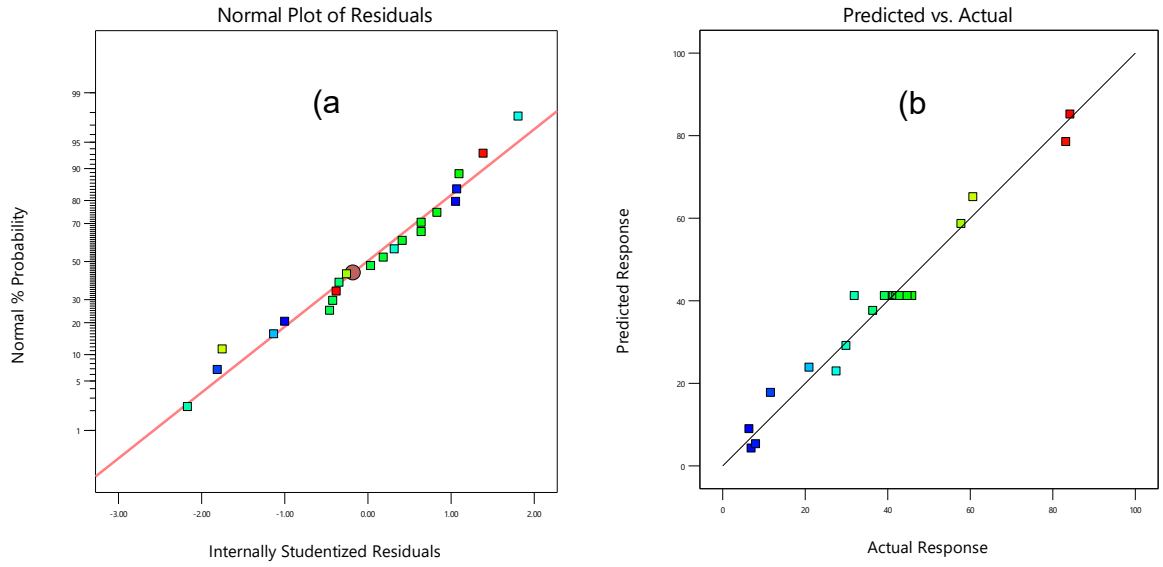

Figure 2. (a) Normal probability plot of the studentized residuals for lead(II) adsorption on SCG, (b) Correlation of actual and predicted removal of lead(II) by SCG.

A normal probability plot was generated to assess the normality of the residuals, as shown in Figure 2(a). The studentized residual was calculated by dividing the residual by an estimate of its standard deviation. The residual values lay roughly between -2 and +2 and closely followed a normal distribution, with most data points aligning well with the fitted line and no significant outliers present. Residuals with values below -2 or above +2 are generally considered large. Ideally, smaller residual values are preferred, as they indicate minimal deviation from the predicted model [31].

The correlation between the actual and predicted responses for lead(II) removal by SCG is illustrated in Figure 2(b). Most of the actual data points lay exactly on or close to the predicted response, indicating that the model was effective in describing the response and could be used for predictions and decision-making within the range of the data. Small deviations between actual and predicted values are typical due to real-world variability and measurement errors. Nevertheless, minimal deviations suggest that the model accurately captured the underlying relationship between the factors and the response.

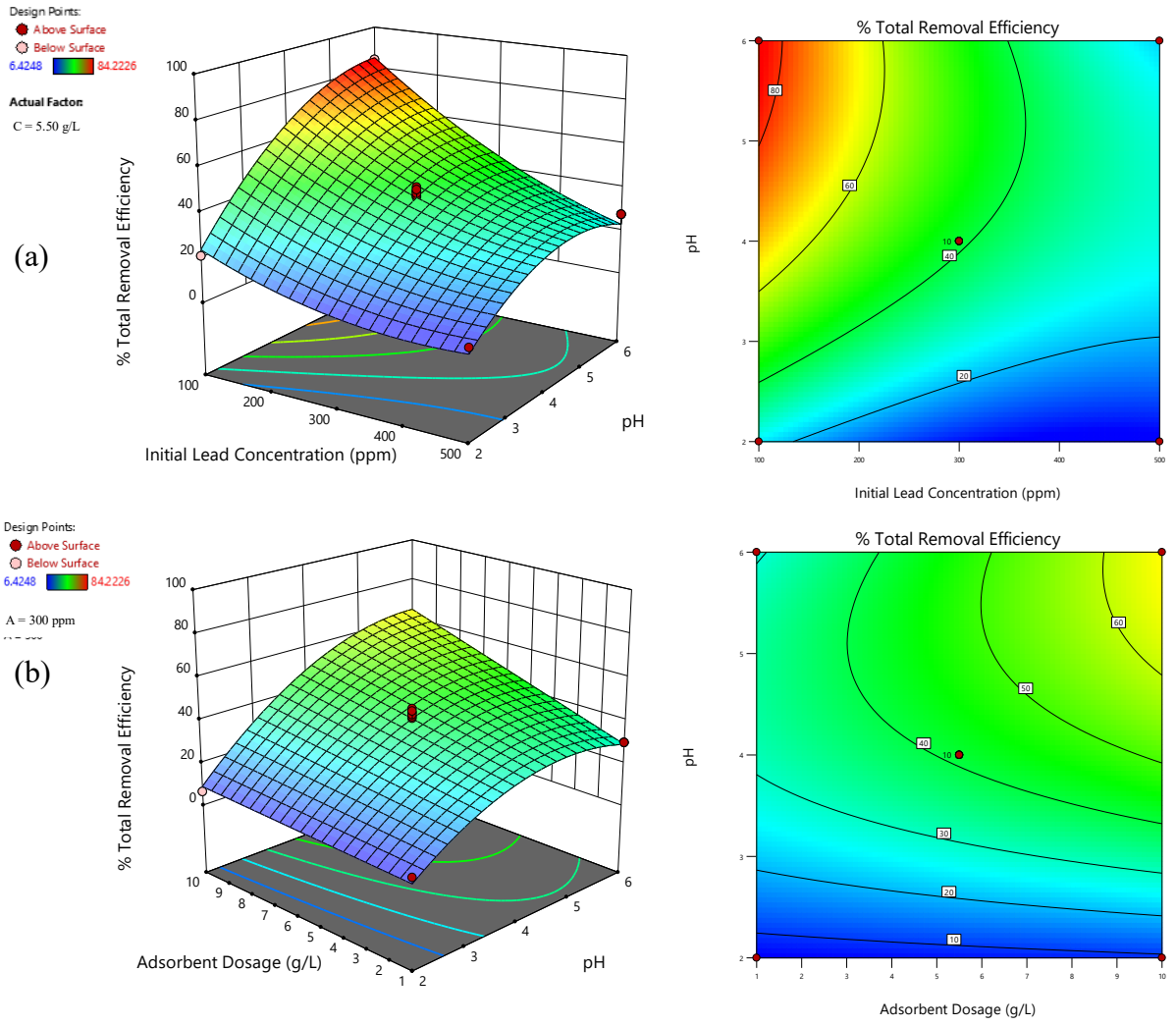

Figure 3. 3D response surface (left) and contour (right) plots of the independent and dependent variables under certain conditions: (a) effect of the interaction of initial lead concentration and pH on lead removal efficiency (%) when the adsorbent dosage was 5.50 g/L, (b) effect of the interaction of the adsorbent dosage and pH on adsorption efficiency (%) when the initial lead concentration was 300 ppm.

Optimization of Lead(II) Adsorption Parameters

The 3D response surface and contour plots for the total lead removal efficiency in relation to both AB and BC interaction are illustrated in Figure 3. The figures show the effects of the interaction of initial lead concentration & pH at a fixed adsorbent dosage of 5.50 g/L, as well as the pH & adsorbent dosage at a fixed initial lead concentration of 300 ppm, on the total lead removal efficiency. The figures indicate that higher removal efficiency could be obtained with a decrease in initial lead concentration and increase in adsorbent dosage. Meanwhile, the effect of pH on the response from both interactions could be seen increasing within the values of the experimental range (pH 2.00-6.00). However, the optimum region was between pH 5.00 and 6.00 because of the presence of curvature. This supports the ANOVA results in which the quadratic term B^2 was found to be significant ($p < 0.05$), implying that the optimal condition was near or within the experimental range of the independent variables.

The optimum conditions for the complete removal of lead(II) from the solution were determined using Stat-Ease 360 software in agreement with the plot analysis. The software established various solutions with their corresponding removal efficiency and desirability. Among these, the solution with the highest total lead removal efficiency and desirability was selected. The optimum conditions were found to be 100 ppm initial lead concentration, a pH of 5.54, and adsorbent dosage of 10.00 g/L. Under these conditions, the predicted total lead removal efficiency was calculated to be 100 %. To validate the model, further experimental trials were conducted in the optimal region to compare the predicted response with practical results, as shown in Table 5. A mean removal efficiency of 97.53 % was obtained in these experiments, with a relative error of 2.47 %, confirming the accuracy of the RSM model. The optimized method was also compared to the negative control (no adsorbent) and positive control (activated carbon) using the method of Abdulkarim and Al-Rub (2003) [32]. No significant difference was observed in their total lead removal efficiency, as shown in Figure 4, indicating the efficiency of the optimized method. The successful application of Response Surface Methodology (RSM) in optimizing the removal of lead(II) from aqueous solutions underscores the novelty of the present study.

Table 5. Experimental validation of predicted values at optimum adsorption conditions.

Optimum conditions[a]	Predicted response (%)	Experimental value (%)*	Relative error[b] (%)
A: 100 ppm B: 5.54 C: 10.00 g/L	100.00	97.53	2.47

[a] – Initial lead concentration, B – pH, C – Adsorbent dosage
[b]–Relative error = [(Pred. value – Exp. value)/Pred. value] x 100%
*-Mean of three replicates

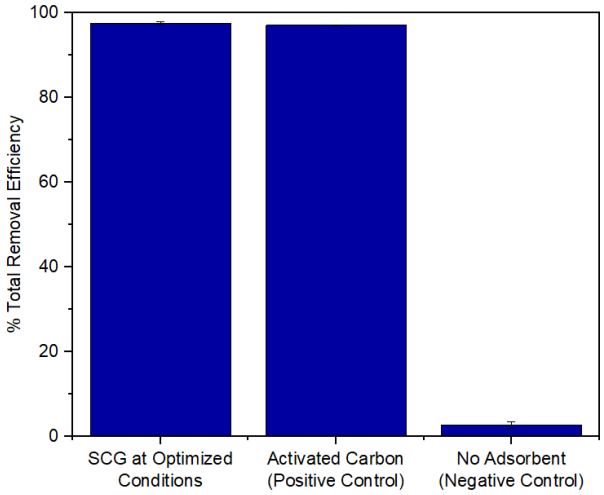

Figure 4. Comparison of % total lead removal efficiency of spent coffee grounds (SCG) at RSM-optimized conditions (adsorbent dosage = 10.00 g/L; initial lead concentration = 100 ppm; pH = 5.54) with activated carbon as the positive control and no adsorbent as the negative control.

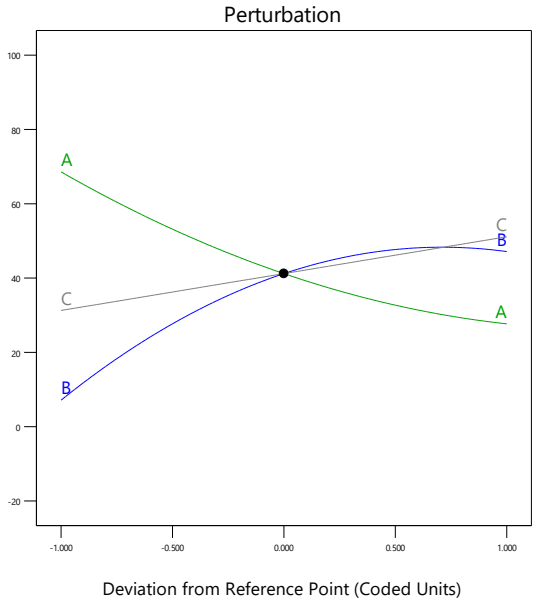

Figure 5. Perturbation plots showing the effects of all independent variables on the response variable: (A) initial lead concentration, (B) pH, and (C) adsorbent dosage.

Effects of Adsorption Parameters on the Response

In addition to the ANOVA results and established equation, the perturbation plot also provides information on how adsorption parameters affected the response, as shown in Figure 5. The presence of a steep slope or curvature indicates that the response variable is highly sensitive to changes in the corresponding parameter, whereas a relatively flat line suggests that the response variable is not significantly affected by variations in that parameter [33, 34]. Among the three independent variables, the initial lead concentration had the greatest impact on the response, followed by pH and adsorbent dosage. Similar findings were observed by several authors, in which they reported initial lead concentration, pH and adsorbent dosage as significant factors in the removal of lead(II) from aqueous solutions using various adsorbents [22, 35, 36].

Effect of Initial Lead(II) Concentration

At low initial concentrations, the number of metal ions available for adsorption is limited, resulting in lower efficiency. As the concentration increases, more ions become available, enhancing the adsorption rate. However, once a certain concentration is reached, the adsorption sites become saturated and can no longer accommodate additional ions [37]. In the present study, high removal efficiency was observed at the lowest initial concentration of 100 ppm as shown in Table 2 and Figure 3, which is contrary to the expected behaviour. However, it is important to note that although this concentration could be the lowest in the experimental design, it may be considered high when compared to any concentration that is less than 100 ppm. The result suggests that at this concentration, the adsorbent's surface could have already been saturated with the adsorbate, and any further increase in concentration could lead to decreased adsorption efficiency and reduced removal of lead(II) from the solution, as was observed in this work. Since complete removal of lead(II) at this concentration was achieved under optimum pH and adsorbent dosage, it can be concluded that all the lead(II) was able to adsorb on the SCG surface.

Effect of pH

The pH of a solution is a critical environmental factor in the adsorption of heavy metal ions, as it heavily influences both the ionization of metal ions and the availability of adsorption sites on the adsorbent surface throughout the process [38]. The key factors influencing pH dependence appear to be the degree to which functional groups become protonated, which in turn leads to electrostatic repulsions between these protonated groups and heavy metal ions [39]. This is usually the case at low pH in which the solubility of lead(II) is high, favouring its retention in the solution. Additionally, as pH decreases, the concentration of H^+ ions increase, which competes with lead(II) for adsorption sites on the surface of SCG. This competition leads to a lower removal efficiency of lead(II) from the solution. Conversely, at higher pH levels, metal ions may form hydroxylated complexes, which can hinder adsorption by blocking the adsorbent's surface [37, 40]. It can be observed from Table 2 and Figure 3 that the experimental runs performed at low pH (pH 2.00) achieved a very low lead removal efficiency which increased with pH. An interesting conclusion is that optimal adsorption was

likely to occur within a moderate pH range [22, 37], which agreed with the optimum pH of 5.54 obtained in this work.

Effect of Adsorbent Dosage

A higher adsorbent dosage improves removal efficiency by providing more adsorption sites for the adsorbate [37, 41, 42]. However, beyond a certain point, a higher dose can cause adsorbents to clump together, reducing the surface area and number of active sites, which in turn lowers adsorption capacity. Thus, increasing adsorbent dosage is advantageous only as long as it provides a greater number of active sites. Beyond this point, efficiency decreases because of agglomeration [37]. The optimized adsorbent dosage in the present work was found to be at the maximum dosage of 10.00 g/L, which indicates that increasing it up to this point still offered a positive effect to the total lead removal efficiency by providing more active sites for the adsorption of lead(II).

SCG Characterization

SCG samples before and after adsorption were subjected to ATR-FTIR and SEM-EDS analysis to confirm the adsorption of lead(II) onto their surfaces.

ATR-FTIR spectroscopy provides information on various functional groups that are present in SCG. Functional groups are crucial in the adsorption of metal ions and determine the adsorption capacity of adsorbents. The quantity and type of functional groups present on the surface of different adsorbents influence the adsorption mechanisms [43, 44]. These functional groups create active sites for the efficient adsorption of heavy metals, with their adsorption potential being affected by several factors [45].

Various functional groups were observed in the ATR-FTIR spectra of SCG before and after adsorption, which provides evidence for their capability to bind with heavy metals such as lead(II). Before adsorption, various peaks were observed as shown in Figure 6. Distinct peaks around 3302, 2922, and 2853 cm^{-1} correspond to the presence of -OH, -CH, and -CH stretching vibrations, respectively. The C=O stretching peaks from 1740-1650 cm^{-1} belong to carbonyl groups of ester and carboxylic acids, while peaks from 1010 to 1155 cm^{-1} represent the -CO stretching due to carboxyl groups of carboxylic acid and ester. Peaks at around 1450 to 1560 were assigned to the C=C stretching of aromatic compounds. These functional groups were due to various components present in SCG such as cellulose, hemicellulose, lignin, fatty acids, and proteins [25]. After adsorption, a decrease in absorbance of functional groups and peak shifts were observed, both due to the adsorption of lead(II) on the surface of SCG. For instance, peaks around 3302.42, 2922.23, 2853.28, 1653.07, and 1155.47 cm^{-1} shifted to 3306.15, 2920.37, 2851.41, 1654.94, and 1153.61 cm^{-1}, respectively, likely due to the complexation of lead(II) with various functional groups. These changes in the ATR-FTIR spectra after the process provided evidence of the adsorption of lead(II) onto the surface of SCG.

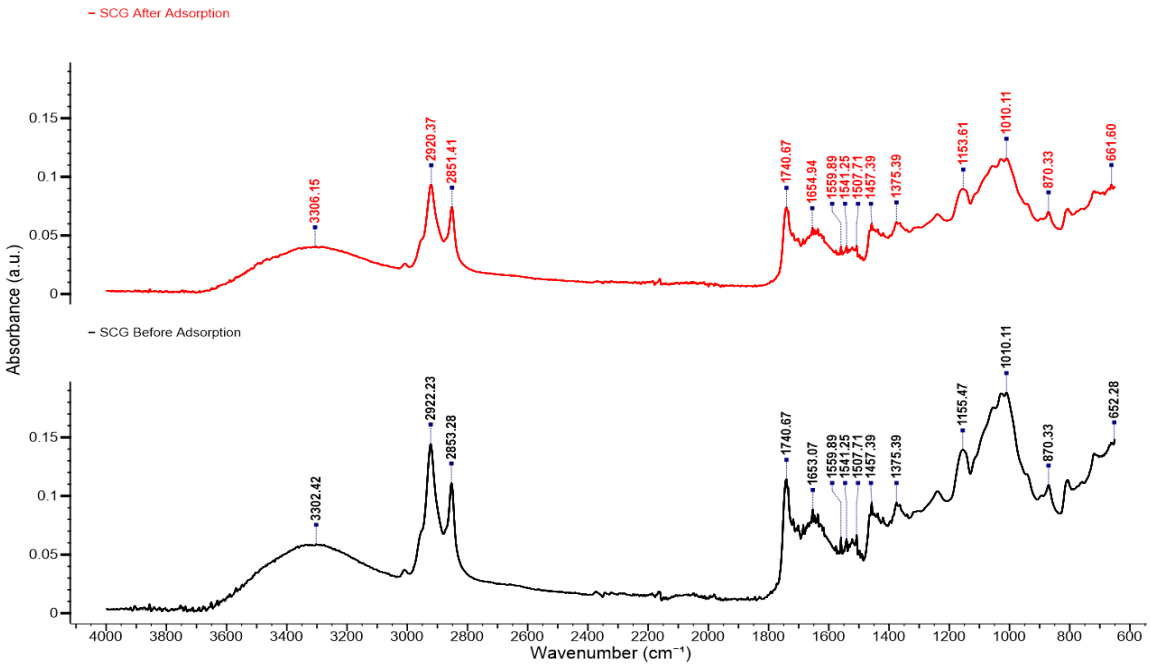

Figure 6. FTIR spectra of SCG before and after lead(II) adsorption, demonstrating changes in functional group absorbances and peak shifts attributable to the interaction of lead(II) ions with the SCG surface. The adsorption experiment was conducted under optimum conditions: adsorbent dosage = 10.00 g/L; initial lead concentration = 100 ppm; pH = 5.54; temperature = 25 °C; contact time = 60 min.

The SEM-EDS analysis provides information on the surface morphology and elemental composition of the sample. In general, adsorption capacity is influenced by several factors such as surface morphology, composition, and porosity, all of which play significant roles [46]. SEM micrographs (Figure 7) revealed that the surface of SCG was relatively uneven, heterogeneous, and contained micropores. Some observed changes in morphological characteristics after adsorption included a slight change in the roughness of surface microstructures. It appears that the SCG had become rougher after adsorption, which is an indication of the adsorption of lead(II) on its surface. EDS results, on the other hand, provided stronger evidence of adsorption, as no lead(II) was detected before the adsorption, as shown in Figure 8. The emergence of peaks that corresponded to lead(II) and its significant contribution to the mass and atom percentages after adsorption, present strong evidence for the adsorption of lead(II) on SCG.

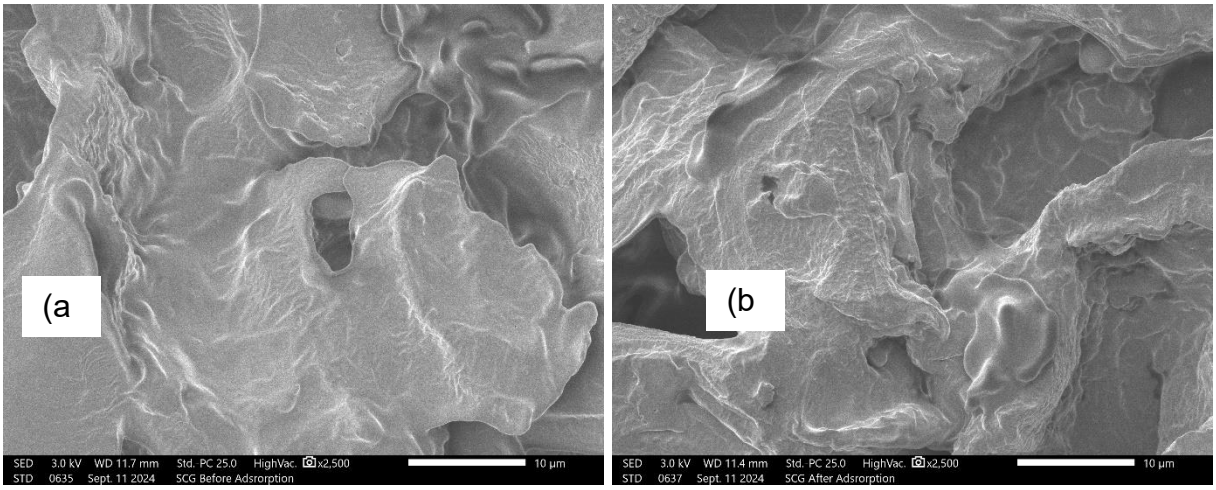

Figure 7. SEM micrographs at 2500x magnification of SCG (a) before, and (b) after lead(II) adsorption, revealing slight changes in surface morphology after the adsorption process. The adsorption experiment was conducted under optimum conditions: adsorbent dosage = 10.00 g/L; initial lead concentration = 100 ppm; pH = 5.54; temperature = 25 °C; contact time = 60 min.

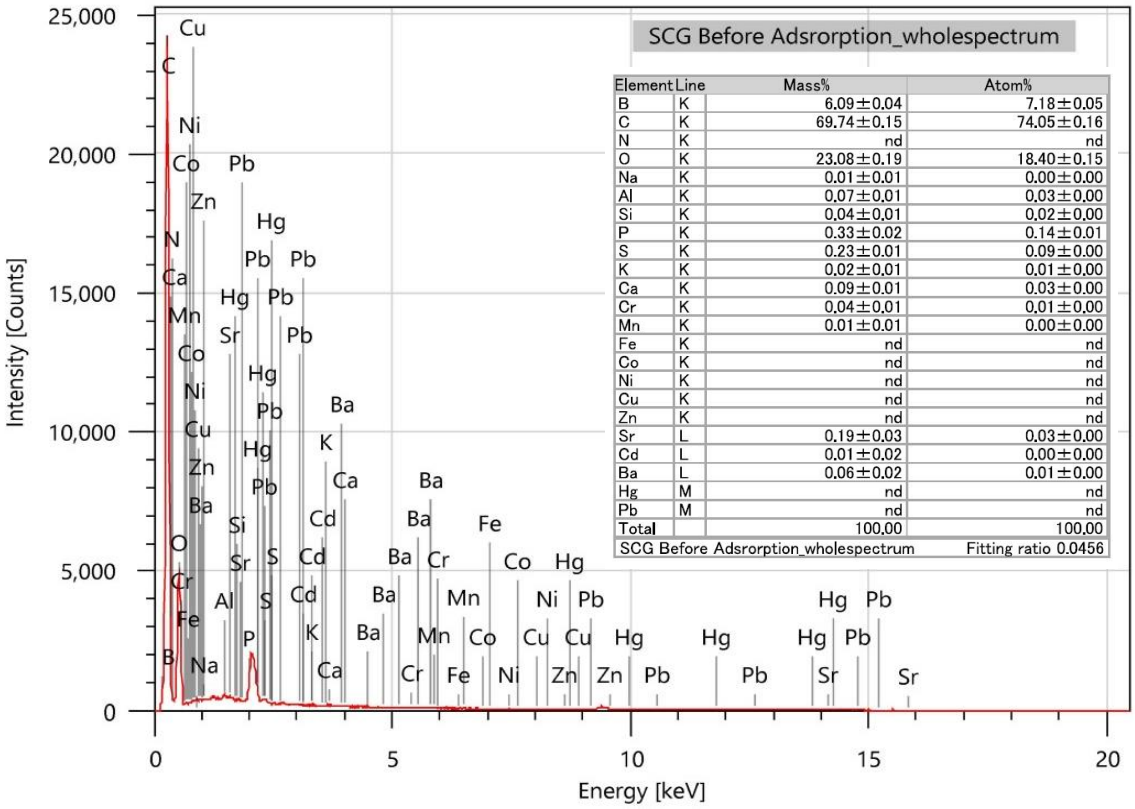

Element	Line	Mass%	Atom%
B	K	6.09±0.04	7.18±0.05
C	K	69.74±0.15	74.05±0.16
N	K	nd	nd
O	K	23.08±0.19	18.40±0.15
Na	K	0.01±0.01	0.00±0.00
Al	K	0.07±0.01	0.03±0.00
Si	K	0.04±0.01	0.02±0.00
P	K	0.33±0.02	0.14±0.01
S	K	0.23±0.01	0.09±0.00
K	K	0.02±0.01	0.01±0.00
Ca	K	0.09±0.01	0.03±0.00
Cr	K	0.04±0.01	0.01±0.00
Mn	K	0.01±0.01	0.00±0.00
Fe	K	nd	nd
Co	K	nd	nd
Ni	K	nd	nd
Cu	K	nd	nd
Zn	K	nd	nd
Sr	L	0.19±0.03	0.03±0.00
Cd	L	0.01±0.02	0.00±0.00
Ba	L	0.06±0.02	0.01±0.00
Hg	M	nd	nd
Pb	M	nd	nd
Total		100.00	100.00
SCG Before Adsrorption_wholespectrum			Fitting ratio 0.0456

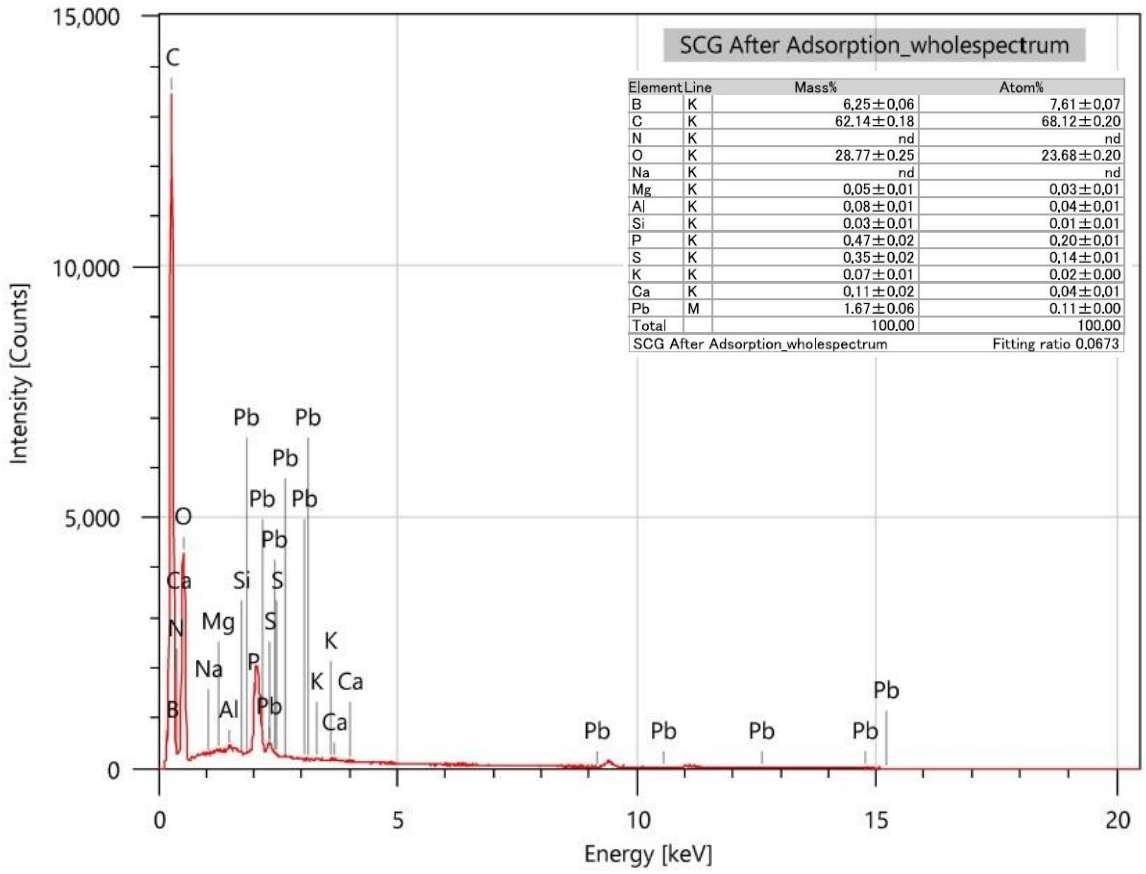

Figure 8. EDS spectra of SCG before and after lead(II) adsorption, illustrating the emergence of lead(II) peaks and corresponding increases in mass and atomic percentages following adsorption. Insets: elemental composition in mass and atom percentages. The adsorption experiment was conducted under optimum conditions: adsorbent dosage = 10.00 g/L; initial lead concentration = 100 ppm; pH = 5.54; temperature = 25 °C; contact time = 60 min.

Adsorption Kinetics

In order to determine the mechanism by which lead(II) adsorbed onto the surface of SCG, adsorption kinetics were analysed using two kinetic models: first-order and pseudo-second-order kinetics [47, 48].

The equation for the Lagergren first-order kinetic model is presented below:

$$\frac{dq_t}{dt} = k_1 (q_e - q_t)$$

where k_1 (1/min) is the first-order rate constant, q_e (mg/g) is the equilibrium uptake and q_t (mg/g) is the uptake at time t. This can be integrated using the boundary condition q_t = 0 at t = 0 to give:

$$\ln(q_e - q_t) = lnq_e - k_1 t$$

The first-order rate constant (k_1) represents the speed at which the adsorption system approaches equilibrium. The parameters q_e and q_t refer to the amount of adsorbate adsorbed at equilibrium and at a given time t, respectively. This model assumes that the rate of occupation of adsorption sites is proportional to the number of unoccupied sites and is governed by a single, rate-limiting step, typically external surface adsorption, commonly associated with physisorption.

If the adsorption kinetics followed the first-order kinetic equation, a plot of ln ($q_e - q_t$) versus t should result in a straight line.

Meanwhile, the equation for the pseudo-second-order kinetic model is presented below:

$$\frac{dq_t}{d_t} = k_2(q_e - q_t)^2$$

where k_2 (g/(mg min) is the pseudo-second-order rate constant. Integrating it with the boundary condition q_t = 0 at t = 0 gives:

$$\frac{t}{q_t} = \frac{t}{q_e} + \frac{1}{k_2\, q_e^2}$$

Similarly, k_2 provides insight into the rate of chemisorption. The parameters q_e and q_t represent the

amount of adsorbate adsorbed at equilibrium and at a specific time t, respectively. This model assumes that the adsorption rate is proportional to the square of the number of available adsorption sites, indicating chemisorption as the rate-limiting step. Additionally, it offers a more accurate prediction of adsorption capacity over a broader time range compared to the pseudo-first-order model.

For pseudo-second-order kinetics, a plot of t/q_t versus t should result in a straight line, with the values of q_e and k_2 being determined from the slope and the intercept.

Figure 9 shows the graph of the pseudo-second-order and first-order kinetic models, yielding R^2 values of 0.99924 and 0.73021, respectively. This indicates that the adsorption of lead(II) onto SCG followed pseudo-second-order kinetics. This model assumes that the rate of adsorption is proportional to the square of the number of unoccupied sites [49]. As shown in Table 6, the theoretical q_e value was 22.32 mg/g, closely matching the experimental value of 21.31 mg/g. This result further confirms that the adsorption process of lead(II) onto the SCG followed a pseudo-second-order reaction mechanism, with the adsorption rate primarily controlled by chemical adsorption, and the chemisorption step acting as the rate-limiting step in the lead(II) adsorption process [50, 51]. Similar findings have been reported regarding the adsorption of metal ions on various adsorbents, such as lead(II) adsorption on *Tamarindus indica* L. [35], Cd(II) adsorption on Turkish SCG [52], and Cd(II), Mn(II), and lead(II) adsorption on SCG and activated SCG [53].

Apart from determining the kinetic model that best described the adsorption of lead(II) onto SCG, the effect of contact time was also analysed to determine the equilibrium time, or the time required for lead(II) and the adsorbent to reach equilibrium. As shown in Figure 10, equilibrium was reached after 60 minutes. The short equilibrium time and rapid adsorbate removal suggest that the adsorbent was highly effective. Adsorption kinetics are typically characterized by two stages. In the first stage, the maximum amount of metal is adsorbed within the initial few minutes, followed by a slower process as the system approaches equilibrium [54, 55]. Since the number of available binding sites is limited, rapid adsorption in the initial stage is expected. However, the adsorption rate declines in the second stage as these sites gradually fill up and residual metal ions compete for the remaining binding sites [56].

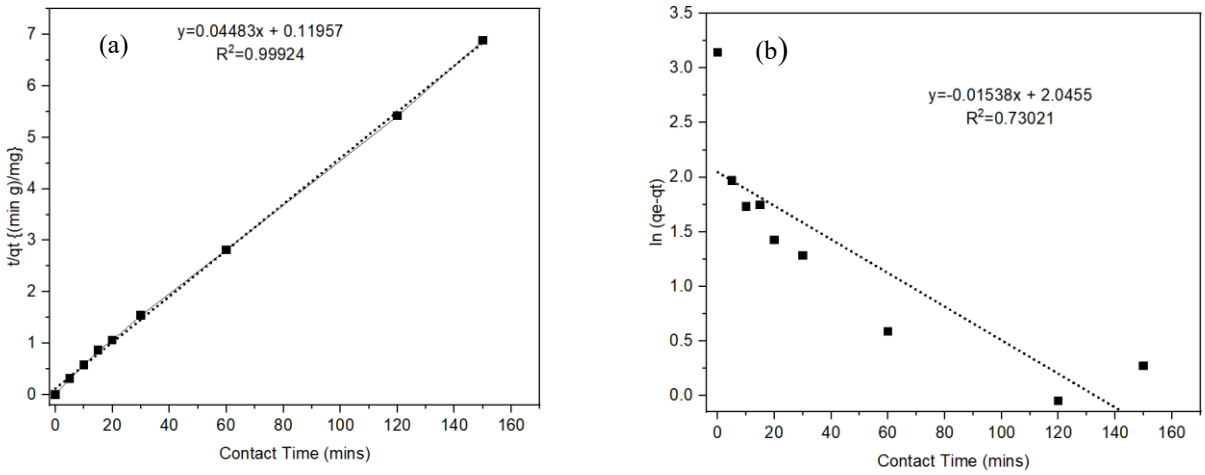

Figure 9. (a) Pseudo-second-order and (b) first-order kinetics of lead(II) ion adsorption onto SCG. Experimental conditions: adsorbent dosage = 10.00 g/L, initial lead concentration = 250 ppm, pH = 5.20, temperature = 25 °C, contact time = 0 to 150 min.

Table 6. Kinetic model parameters for lead(II) adsorption onto SCG.

Initial lead(II) concentration (mg/L)	q_e (exp) (mg/g)	First-order model			Pseudo-second-order model		
		q_e (cal) (mg/g)	k_1 (1/min)	R^2	q_e (cal) (mg/g)	k_2 [g/(mg min)]	R^2
250	21.31	7.73	0.0154	0.7302	22.32	0.01678	0.9992

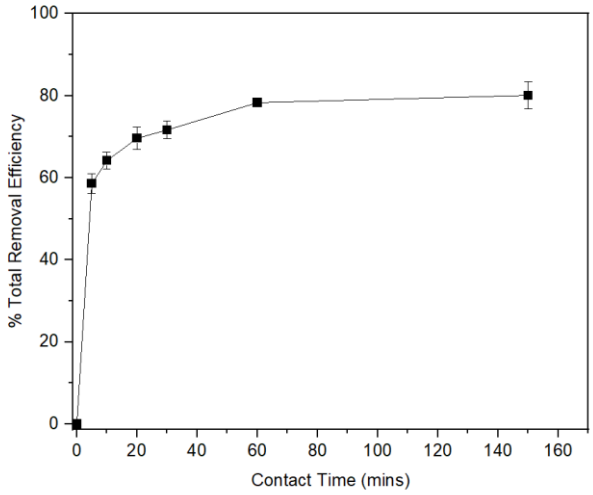

Figure 10. Effect of contact time on the % total lead removal efficiency of spent coffee grounds. Experimental conditions: adsorbent dosage = 10.00 g/L, initial lead concentration = 250 ppm, pH = 5.20, temperature = 25 °C, contact time = 0 to 150 min.

Adsorption Isotherms

Equilibrium adsorption isotherms are important parameters for assessing the adsorption capacity of adsorbents and understanding the mechanisms involved in the adsorption process. Here, two equilibrium adsorption isotherm models, Langmuir and Freundlich, were used to evaluate the adsorption process of lead(II) onto SCG. The former assumes a homogenous monolayer adsorption onto the adsorbent and proposes that the adsorption energy is the same throughout the surface [51], while the latter assumes a heterogenous multilayer adsorption and that the adsorption energies are not uniformly distributed throughout the surface [57].

The Langmuir isotherm equation can be written as: [32]

$$\frac{C_e}{q_e} = \frac{1}{q_m b} + \frac{C_e}{q_m}$$

where C_e is the equilibrium concentration (in mg/L), q_e represents the amount of metal ions adsorbed (in mg/g) at equilibrium, q_m corresponds to the maximum monolayer capacity of the adsorbent (in mg/g), and b is the adsorption constant (in L/mg) or the affinity of the binding sites for the adsorbate, wherein a higher b value indicates stronger binding. According to this equation, plotting C_e/q_e against C_e produces a straight line, where the slope is $1/q_m$ and the intercept is $1/q_m$b.

The Freundlich isotherm equation, on the other hand, can be written as: [32]

$$lnq_e = lnK + \frac{1}{n} lnC_e$$

where C_e and q_e are the same as the above, while K and 1/n are the Freundlich isotherm constants that correspond to adsorption capacity and adsorption density, respectively. A higher value for adsorption capacity suggests greater adsorption ability, while adsorption density values of $0<1/n<1$ and $1/n>1$ indicate favourable and poor adsorption, respectively. According to this equation, plotting $\ln q_e$ against $\ln C_e$ produces a straight line, where the slope is 1/n and the intercept is lnK.

Each model was evaluated based on their R^2 value, in which the model that obtained a better R^2 was used to describe the isotherm mechanism for the adsorption of lead(II) onto SCG. Based on Figure 11, the two models had R^2 values that were relatively close to each other. However, the Langmuir isotherm gave a better fit as evident from its high R^2 value of 0.99928, indicating that this model was more suitable to explain the adsorption properties of lead(II) and SCG. Thus, the present work suggests a monolayer adsorption of lead(II) on the surface of SCG.

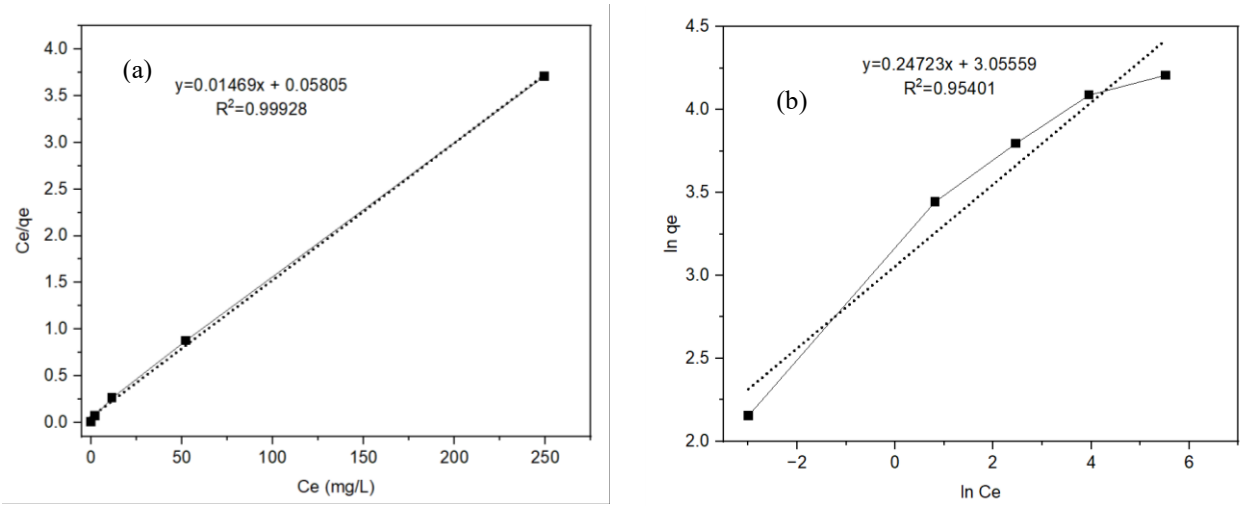

Figure 11. (a) Linearized Langmuir and (b) Freundlich adsorption isotherms for lead(II) ions on SCG. Experimental conditions: adsorbent dosage = 1.00 g/L, pH = 5.20, temperature = 25 °C, contact time = 60 min, initial lead concentration = 10 to 250 ppm.

Table 7. Isotherm model parameters for lead(II) adsorption onto SCG.

Freundlich			Langmuir			
K	1/n	R^2	q_m (mg/g)	b (L/mg)	R^2	R_L range
21.23	0.2472	0.95401	68.03	0.2534	0.99928	0.3127-0.0123

The lead(II) adsorption capacity of SCG (q_m), as shown in Table 7, was calculated to be 68.03 mg/g. This was much higher compared to the results of previous reports that also used SCG [25, 26, 53, 58, 61, 62] and other adsorbents [35, 59, 60]. For instance, Lavecchia et al. (2016) [25] and Chwastowski et al. (2020) [53] obtained a maximum adsorption capacity of 2.46 and 46.29 mg/g, respectively for the removal of lead(II) using SCG. In addition, one study reported that SCG treated with $Ca(OH)_2$ under optimized conditions (contact time of 270 min, pH 6.00, adsorbent dosage of 1.00 g, and temperature of 40 °C) achieved a maximum adsorption capacity of 18.69 mg/g for lead(II) ions [61]. Lastly, an investigation using biosorbents derived from locally sourced *Robusta* SCG, carbonized at 400 °C and activated with 0.20 M HCl, demonstrated an adsorption capacity of 8.6683 mg/g for lead(II), corresponding to a lead removal efficiency of 51.60 % under ambient temperature conditions [62]. Meanwhile, the b value and separation factor (R_L) range were calculated to be 0.2534 L/mg and 0.3127-0.0123, respectively. R_L values between 0-1 indicate favourable adsorption between adsorbate and adsorbent [63]. The present work, therefore, demonstrates SCG as a potential adsorbent for the removal of lead(II) from aqueous solutions.

CONCLUSION

The present study found that untreated SCG was a low-cost, sustainable, eco-friendly and promising adsorbent for the removal of lead(II) from aqueous solutions. RSM based on BBD was successfully employed for the optimization of lead(II) removal from aqueous solutions. Adsorption parameters such as initial lead concentration, pH, and adsorbent dosage were investigated to determine their effects on the total lead removal efficiency of SCG. All parameters were found to be significant ($p<0.05$) and thus exerted positive impacts on the adsorption process. Significant higher-order interactions were also observed in the model, specifically between initial lead concentration & pH, and adsorbent dosage & pH. The optimum conditions established using RSM were 100 ppm initial lead concentration, pH of 5.54, and 10.00 g/L of adsorbent dosage. The predicted response under these conditions was 100 % lead removal efficiency. A mean response of 97.53 % was obtained in the experimental trials, leaving a relative error of 2.47 %, which therefore validated the reliability of the established RSM model (R^2=0.9701). The removal efficiency of SCG under optimum conditions was comparable to the positive control (activated carbon) that achieved a 97.05 % removal efficiency.

The presence of lead(II) on the SCG surface after adsorption was confirmed by ATR-FTIR and SEM-EDS analyses. ATR-FTIR spectra showed the presence of various functional groups that participate in metal binding. After adsorption, a decrease in absorbance and slight shifts in the functional groups peaks were observed, which may be due to the complexation of functional groups with lead(II). EDS also revealed the presence of lead(II) after adsorption by the emergence of characteristic lead(II) peaks on the EDS spectra, which contributed to the overall percentage elemental composition of SCG.

Adsorption kinetics was consistent with a pseudo-second-order kinetic model (R^2=0.99924), indicating that adsorption was mainly controlled by chemical adsorption, based on the influence of valence forces through sharing or exchange of electrons between lead(II) and the SCG surface. It also indicated that the rate of adsorption was proportional to the square of the number of available adsorption sites.

The adsorption isotherm was best described by a Langmuir isotherm model (R^2=0.99928), which indicated a monolayer adsorption of lead(II) onto the SCG surface. Based on this model, the lead(II) adsorption capacity of SCG was 68.03 mg/g, demonstrating its promising potential as an adsorbent for the removal of lead(II) from aqueous solutions.

Future studies should investigate the reusability of SCG and the scalability of the process, emphasizing challenges like material regeneration and the long-term stability of the adsorbent.

ACKNOWLEDGEMENTS

The author expresses his sincere thanks to the following: (1) the Cordillera Studies Center, University of the Philippines Baguio, for funding and supporting this work; (2) the Department of Physical Sciences, University of the Philippines Baguio, for providing laboratory space for this study; (3) the Regional Soils Laboratory, Department of Agriculture Regional Field Office 3, for their assistance with AAS analysis; and (4) the Central Instrumentation Facility, De La Salle University, for their services in ATR-FTIR and SEM-EDS analysis. The author also extends his gratitude to Mr. John Paulo A. Samin and Mr. Justine O. Estabillo for the technical assistance they provided during this work.

REFERENCES

1. Gill, J. C., Mankelow, J. and Mills, K. (2019) The role of Earth and environmental science in addressing sustainable development priorities in Eastern Africa. *Environmental Development*, **30**, 3–20.

2. UN-WATER (2020) United Nations World Water Development Report 2020: Water and Climate Change. *UNESCO, Paris, France*. https://www.unwater. org/publications/world-water-development-report-2020 (Accessed: 15 March 2024).

3. Boretti, A. and Rosa, L. (2019) Reassessing the projections of the World Water Development Report. *NPJ Clean Water*, **2(1)**, 15.

4. Kummu, M., Guillaume, J. H., de Moel, H., Eisner, S., Flörke, M., Porkka, M., Siebert, S., Veldkamp, T. I. and Ward, P. J. (2016) The world's road to water scarcity: shortage and stress in the 20th century and pathways towards sustainability. *Scientific Reports*, **6**, 38495.

5. Mekonnen, M. M. and Hoekstra, A. Y. (2016) Four billion people facing severe water scarcity. *Science Advances*, **2**, e1500323.

6. Fu, Z. and Xi, S. (2020) The effects of heavy metals on human metabolism. *Toxicology Mechanisms and Methods*, **30(3)**, 167–176.

7. Amarasinghe, B. M. W. P. K. and Williams, R. A. (2007) Tea waste as a low-cost adsorbent for the removal of Cu and Pb from wastewater. *Chemical Engineering Journal*, **132(1–3)**, 299–309.

8. Ronteltap, M., Maurer, M. and Gujer, W. (2007) The behaviour of pharmaceuticals and heavy metals during struvite precipitation in urine. *Water Research*, **41**, 1859–1868.

9. Aklil, A., Mouflih, M. and Sebti, S. (2004) Removal of heavy metal ions from water by using calcined phosphate as a new adsorbent. *Journal of Hazardous Materials*, **112(3)**, 183–190.

10. Duraipandian, J., Rengasamy, T. and Vadivelu, S. (2017) Experimental and modeling studies for the removal of crystal violet dye from aqueous solutions using eco-friendly Gracilaria corticata seaweed activated carbon/Zn/Alginate polymeric composite beads. *Journal of Polymers and the Environment*, **25**, 1062–1071.

11. Zhang, X., Lin, S., Lu, X. Q. and Chen, Z. L. (2010) Removal of Pb(II) from water using synthesized kaolin supported nanoscale zero-valent iron. *Chemical Engineering Journal*, **163**, 243–248.

12. Jazi, M. B., Arshadi, M., Amiri, M. J. and Gil, A. (2014) Kinetic and thermodynamic investigations of Pb(II) and Cd(II) adsorption on nanoscale organo-functionalized $SiO_2Al_2O_3$. *Journal of Colloid and Interface Science*, **422**, 16–24.

13. Kim, M. S. and Kim, J. G. (2020) Adsorption characteristics of spent coffee grounds as an alternative adsorbent for cadmium in solution. *Environments*, **7(4)**, 24.

14. International Coffee Organization (2023) Coffee Report and Outlook (CRO). https://icocoffee.org/documents/cy2022-23/Coffee_Report_and_Outlook_April_2023_-_ICO.pdf (Accessed 28 September 2024).

15. Liang, S. L., Guo, X. Y. and Tian, Q. H. (2011) Adsorption of Pb^{2+} and Zn^{2+} from aqueous solutions by sulfured orange peel. *Journal of Hazardous Materials*, **174**, 756–762.

16. Sun, S., Yang, J., Li, Y., Wang, K. and Li, X. (2014) Optimizing adsorption of Pb(II) by modified litchi pericarp using the response surface methodology. *Ecotoxicology and Environmental Safety*, **108**, 29–35.

17. Bulatao, R. M., Samin, J. P. A., Tubera, R. P., Rubio, M. M. M., Romano, D. C. and Rafael, R. R. (2019) Optimization of process parameters for the extraction of anthocyanins from black rice bran using response surface methodology. *The Philippine Agricultural Scientist*, **102(1)**, 1–12.

18. Yolmeh, M. and Jafari, S. M. (2017) Applications of response surface methodology in the food industry processes. *Food and Bioprocess Technology*, **10**, 413–433.

19. Said, K. A. M. and Amin, M. A. M. (2015) Overview on the response surface methodology (RSM) in extraction processes. *Journal of Applied Science and Process Engineering*, **2**, 8–17.

20. Gu, F., Xu, F., Tan, L., Wu, H., Chu, Z. and Wang, Q. (2012) Optimization of enzymatic process for vanillin extraction using response surface methodology. *Molecules*, **17(8)**, 8753–8761.

21. Kuo, C. H., Hsiao, F. W., Chen, J. H., Hsieh, C. W., Liu, Y. C. and Shieh, C. J. (2013) Kinetic aspects of ultrasound-accelerated lipase catalyzed acetylation and optimal synthesis of 4′-acetoxyresveratrol. *Ultrasonics Sonochemistry*, **20**, 546–552.

22. Rezaei, M., Pourang, N. and Moradi, A. M. (2022) Removal of lead from aqueous solutions using three biosorbents of aquatic origin with the emphasis on the effective factors. *Scientific Reports*, **12**, 751.

23. Bahrami, M., Amiri, M. J. and Bagheri, F. (2019) Optimization of the lead removal from aqueous solution using two starch-based adsorbents: Design of experiments using response surface methodology (RSM), *Journal of Environmental Chemical Engineering*, **7(1)**, 102793.

24. Antonio, J. B, Malapit, G., Mendoza, J. P. and Valdez, J. (2022) Lead (Pb^{2+}) removal in water using different forms of spent Arabica coffee grounds at varying contact time. *E3S Web of Conferences*, **355**, 02001.

25. Lavecchia, R., Medici, F., Patterer, S. and Zuorro, A. (2016) Lead removal from water by adsorption on spent coffee grounds. *Chemical Engineering Transactions*, **47**, 295–300.

26. Futalan, C. M., Kim, J. and Yee, J. J. (2019) Adsorptive treatment via simultaneous removal of copper, lead and zinc from soil washing wastewater using spent coffee grounds. *Water Science and Technology*, **79(6)**, 1029–1041.

27. Li, M., Feng, C., Zhang, Z., Chen, R., Xue, Q., Gao, C. and Sugiura, N. (2010) Optimization of process parameters for electrochemical nitrate removal using Box–Behnken design. *Electrochimica Acta*, **56**, 265–270.

28. Montgomery, D. C. (2017) Design and Analysis of Experiments. *Wiley, New York*.

29. Amini, M., Younesi, H., Bahramifar, N., Lorestani, A. A., Ghorbani, F., Daneshi, A. and Sharifzadeh, M. (2008) Application of response surface methodology for optimization of lead biosorption in an aqueous solution by *Aspergillus niger*. *Journal of Hazardous Materials*, **154(1–3)**, 694–702.

30. Zar, J. H. (2010) Biostatistical Analysis, 5th eds. Prentice Hall, New Jersey.

31. Anuar, N., Mohd Adnan, A. F., Saat, N., Aziz, N. and Mat Taha, R. (2013) Optimization of extraction parameters by using response surface methodology, purification, and identification of anthocyanin pigments in *Melastoma malabathricum* fruit. *The Scientific World Journal*, **2013(1)**, 810547.

32. Abdulkarim, M. and Al-Rub, F. A. (2004) Adsorption of lead ions from aqueous solution onto activated carbon and chemically-modified activated carbon prepared from date pits. *Adsorption Science & Technology*, **22(2)**, 119–134.

33. Anderson, M. J. and Whitcomb, P. J. (2016) RSM simplified: Optimizing processes using response surface methods for design of experiments. *Productivity Press, Boca Raton*.

34. Myers, R. H., Montgomery, D. C. and Anderson-Cook, C. M. (2016) Response Surface

Methodology: Process and Product Optimization Using Designed Experiments. *Wiley, New York*.

35. Bangaraiah, P. and Sarathbabu, B. (2019) Optimization of process parameters in removal of lead from aqueous solution through response surface methodology. *Chemical Engineering Communications*, **206(8)**, 986–993.

36. Javanbakht, V. and Ghoreishi, S. M. (2017) Application of response surface methodology for optimization of lead removal from an aqueous solution by a novel superparamagnetic nano-composite. *Adsorption Science & Technology*, **35(1–2)**, 241–260.

37. Singh, S., Kapoor, D., Khasnabis, S., Singh, J. and Ramamurthy, P. C. (2021) Mechanism and kinetics of adsorption and removal of heavy metals from wastewater using nanomaterials. *Environmental Chemistry Letters*, **19**, 2351–2381.

38. Abbar, B., Alem, A., Marcotte, S., Pantet, A., Ahfir, N. D., Bizet, L. and Duriatti, D. (2017) Experimental investigation on removal of heavy metals (Cu^{2+}, Pb^{2+}, and Zn^{2+}) from aqueous solution by flax fibres. *Process Safety and Environmental Protection*, **109**, 639–647.

39. Fu, F., Ma, J., Xie, L., Tang, B., Han, W. and Lin, S. (2013) Chromium removal using resin supported nanoscale zero-valent iron. *Journal of Environmental Management*, **128**, 822–827.

40. Wadhawan, S., Jain, A., Nayyar, J. and Mehta, S. K. (2020) Role of nanomaterials as adsorbents in heavy metal ion removal from wastewater: a review. *Journal of Water Process Engineering*, **33**, 101038.

41. Al-Saeedi, J. Y., Akbar, M. M. and Al-Qarooni, I. H. (2019) Removal of Pb(II) and Ni(II) ions from aqueous solution by sea snail shells. *Journal of Biodiversity and Environmental Sciences*, **14(3)**, 17–23.

42. Osu, C. I. and Odoemelam, S. A. (2010) Studies on adsorbent dosage, particle sizes and pH constraints on biosorption of Pb(II) and Cd(II) ions from aqueous solution using modified and unmodified *Crasstrotrea Gasar* (bivalve) biomass. *Journal of Hazardous Materials*, **174**, 500–505.

43. Gupta, V. G., Treichel, H., Kuhad, R. C. and Rodriguez-Couto, S. (2020) Recent Developments in Bioenergy Research. *Springer, Berlin*.

44. Sooksawat, N., Meetam, M., Kruatrachue, M., Pokethitiyook, P. and Inthorn, D. (2017) Performance of packed bed column using *Chara aculeolata* biomass for removal of Pb and Cd ions from wastewater. *Journal of Environmental Science and Health, Part A*, **52**, 539–546.

45. Andal, N. M., Charulatha, S., Gayathri, N. S. and Anuradha, J. (2016) A comparative study on the sorption of divalent ions by bivalves shells: Equilibrium and statistical studies. *Chemical Science Review and Letters*, **5(19)**, 214–223.

46. Parida, U., Bastia, T. K. and Kar, B. B. (2017) A study on the water absorption efficiency of porous silica gel prepared from rice husk ash. *Asian Journal of Water, Environment and Pollution*, **14**, 83–86.

47. Benjelloun, M., Miyah, Y., Evrendilek, G. A., Zerrouq, F. and Lairini, S. (2021) Recent advances in adsorption kinetic models: their application to dye types. *Arabian Journal of Chemistry*, **14(4)**, 103031.

48. Yoosefian, M., Ahmadzadeh, S., Aghasi, M. and Dolatabadi, M. (2017) Optimization of electro-coagulation process for efficient removal of ciprofloxacin antibiotic using iron electrode; kinetic and isotherm studies of adsorption. *Journal of Molecular Liquids*, **225**, 544–553.

49. Liang, S., Guo, X., Feng, N. and Tian, Q. (2010) Isotherms, kinetics and thermodynamic studies of adsorption of Cu^{2+} from aqueous solutions by Mg^{2+}/K^{+} type orange peel adsorbents. *Journal of Hazardous Materials*, **174**, 756–762.

50. Ho, Y. S. and McKay, G. (1998) A comparison of chemisorption kinetic models applied to pollutant removal on various sorbents. *Process Safety and Environmental Protection*, **76(4)**, 332–340.

51. Shami, R. B., Shojaei, V. and Khoshdast, H. (2019) Efficient cadmium removal from aqueous solutions using a sample coal waste activated by rhamnolipid biosurfactant. *Journal of Environmental Management*, **231**, 1182–1192.

52. Delil, A. D., Gülçiçek, O. and Gören, N. (2019) Optimization of adsorption for the removal of cadmium from aqueous solution using Turkish coffee grounds. *International Journal of Environmental Research*, **13**, 861–878.

53. Chwastowski, J., Bradło, D. and Żukowski, W. (2020) Adsorption of cadmium, manganese and lead ions from aqueous solutions using spent coffee grounds and biochar produced by its pyrolysis in the fluidized bed reactor. *Materials*, **13(12)**, 2782.

54. Panda, G. C., Das, S. K., Bandopadhyay, T. S. and Guha, A. K. (2007) Adsorption of nickel on husk of *Lathyrus sativus*: behavior and

binding mechanism. *Colloids and Surfaces B: Biointerfaces*, **57**, 135–142.

55. Saeed, A., Iqbal, M. and Akhtar, M. W. (2005) Removal and recovery of lead (II) from single and multimetal (Cd, Cu, Ni, Zn) solutions by crop milling waste (black gram husk), *Journal of Hazardous Materials*, **117**, 65–73.

56. Basu, M., Guha, A. K. and Ray, L. (2017) Adsorption behavior of cadmium on husk of lentil. *Process Safety and Environmental Protection*, **106**, 11–22.

57. Su, C. X. H., Teng, T. T., Alkarkhi, A. F. and Low, L. W. (2014) *Imperata cylindrica* (cogongrass) as an adsorbent for methylene blue dye removal: process optimization. *Water, Air, and Soil Pollution*, **225**, 1–12.

58. Gomez-Gonzalez, R., Cerino-Córdova, F. J., Garcia-León, A. M., Soto-Regalado, E., Davila-Guzman, N. E. and Salazar-Rabago, J. J. (2016) Lead biosorption onto coffee grounds: comparative analysis of several optimization techniques using equilibrium adsorption models and ANN. *Journal of the Taiwan Institute of Chemical Engineers*, **68**, 201–210.

59. Turkyilmaz, H., Kartal, T. and Yigitarslan Yildiz, S. (2014) Optimization of lead adsorption of mordenite by response surface methodology: characterization and modification. *Journal of Environmental Health Science and Engineering*, **12(1)**, 5.

60. Goel, J., Kadirvelu, K., Rajagopal, C. and Garg, V. K. (2005) Removal of lead (II) from aqueous solution by adsorption on carbon aerogel using a response surface methodological approach. *Industrial & Engineering Chemistry Research*, **44(7)**, 1987–1994.

61. Nguyen, T. A., Oanh, D. T. Y., Nguyen, T. T. P., Nguyen, M. H., Nguyen, T. H., Bui, T. T. T. and Hoang, T. D. (2025) Exploring sustainable solutions: utilizing recycled coffee grounds as a new bio-adsorbent material for removal of Pb(II) ions from water. *Vietnam Journal of Chemistry*, **63(2)**, 234–252.

62. Ayucitra, A., Gunarto, C., Kurniawan, V. and Hartono, S. B. (2017) Preparation and characterisation of biosorbent from local Robusta spent coffee grounds for heavy metal adsorption. *Chemical Engineering Transactions*, **56**, 1441–1446.

63. Badi, M. Y., Azari, A., Pasalari, H., Esrafili, A. and Farzadkia, M. (2018) Modification of activated carbon with magnetic Fe_3O_4 nano-particle composite for removal of ceftriaxone from aquatic solutions. *Journal of Molecular Liquids*, **261**, 146–154.